

Structure of the solid D₂ bilayer on graphite

Wei Liu and S. C. Fain, Jr.

Department of Physics, University of Washington, Seattle, Washington 98195

(Received 29 October 1992)

Low-energy electron-diffraction (LEED) measurements for a solid D₂ bilayer physisorbed on graphite are used to investigate the bilayer structure and its azimuthal orientation relative to the substrate. The LEED spot positions are consistent with the mutually commensurate oblique unit cell inferred from neutron-diffraction measurement. Given the azimuthal orientation of the bilayer LEED spots, the possibility of a bilayer composed of two incommensurate layers with mutually modulated triangular lattices is ruled out.

The growth and structure of multilayer films physisorbed on graphite are active areas of study.¹⁻⁶ The competition between adsorbate-substrate, intralayer and interlayer adsorbate-adsorbate interactions plays a crucial role in the various commensurability transitions in multilayers.¹ It is particularly interesting to study the bilayer structure of quantum systems such as ⁴He, ³He, H₂, HD, and D₂ physisorbed on graphite, considering their large quantum zero-point motion and high compressibility that may lead to the growth of a limited number of solid or fluid layers. Recent neutron-diffraction studies show that for ⁴He on graphite^{2,3} the bilayer has two independent triangular unit cells with the second layer being less closely packed than and incommensurate with the first layer. In contrast, the D₂ bilayer on graphite^{4,5} has two mutually commensurate layers and adopts a common oblique cell at $T < 15$ K. By fitting a powder-averaged Lorentzian-squared line shape to the peak positions as well as intensities, Wiechert and co-workers^{4,5} have inferred the lattice parameters of the oblique unit cell. In spite of this success, the possibility of two mutually incommensurate triangular layers modulated by each other was not explicitly discussed in these studies. Moreover, the azimuthal orientation of the bilayer relative to the coexisting monolayer and to the substrate has not been ascertained by the neutron diffraction because of the use of powder samples. It is well known that low-energy electron diffraction (LEED) has the advantage over neutron diffraction of using single crystals, and is sensitive to the azimuthal orientation. In this paper, we report our LEED measurements on the D₂ bilayer on graphite single crystals. Our results confirm the oblique structure proposed by the neutron-diffraction studies. We also observe the definite orientation of the bilayers with respect to the monolayer triangular lattice and to the substrate. On the basis of this observation, we prove that the weakest of the three neutron-diffraction peaks^{4,5} cannot be interpreted as a satellite due to the modulation between two mutually incommensurate triangular lattices.⁶

The basic LEED apparatus and experimental procedures have been described previously.^{7,8} Briefly, the overall resolution at the electron energy of 63.2 eV for optimizing the D₂ patterns is 0.04 \AA^{-1} full width at half

maximum (FWHM). The electron beam was deflected away from the sample most of the time except while an image was being taken. Each LEED image is the average over five consecutive frames with a total electron exposure of 1.5 nA for 0.9 sec. As the substrate was cooled to $T \approx 5$ K, the D₂ gas was introduced into the ultrahigh-vacuum system through the effusion tube. The D₂ flux was finely tuned by a leak valve and monitored by a mass spectrometer. A series of D₂ monolayer structures as described by Cui and co-workers^{7,9} have been reproduced as the D₂ flux was gradually increased. The crystal quality was not as good as in the previous work as judged from the range of densities present for an individual LEED pattern for lower fluxes, but it was still good enough to ignore any induced artifact on the bilayer LEED patterns.¹⁰

To ensure any impurity adsorption effect was negligible, we raised the sample temperature and observed that the LEED patterns of the adsorbate disappeared at $T \approx 18$ K. From our experience the only LEED patterns that disappear around this temperature due to thermal desorption are those of hydrogen and its isotopes. The possibility of H₂ and HD impurities in the D₂ LEED patterns cannot be ruled out by this simple test, but is unlikely due to the infrared-induced desorption being much faster for H₂ and HD than for D₂.⁸

The LEED patterns from the D₂ monolayer and bilayer are summarized in Figs. 1 and 2. Figure 1 shows a sequence of LEED photos taken at a fixed temperature at 4.5 K with the D₂ flux adjusted to give from one to two monolayers. The dark region at the center of each pattern is due to the drift tube of the electron gun; the shadow at the top left corner, which blocks one group of the spots, is from the effusion tube. The six groups of six spots for the monolayer rotated incommensurate (RIC) structure [see Figs. 1(a), 1(b), and 2] are explained by two rotation directions and double scattering.⁷ As the flux was increased beyond that for the densest monolayer reached at $q = 2.12 \text{ \AA}^{-1}$, as shown in Fig. 1(a), a set of arclike spots emerges and increases in intensity at $q = 1.97 \text{ \AA}^{-1}$, and the outer spots evolve to arclike spots located at $q = 2.15 \text{ \AA}^{-1}$, as shown in Fig. 1(b) for the coexistence of monolayer and bilayer.

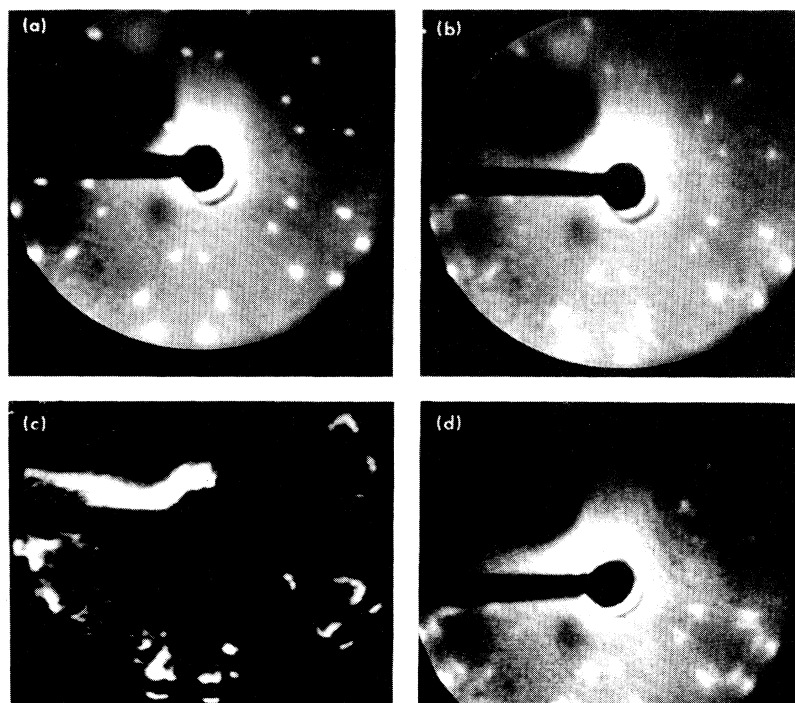


FIG. 1. Photograph of LEED patterns near 4.5 K for 63.2-eV electron energy. (a) Rotated incommensurate triangular solid phase near monolayer completion with the lattice constant $d=3.41\pm 0.04 \text{ \AA}^{-1}$ and the rotational angle $\theta=(7.2\pm 0.5)^\circ$. (b) Coexistence of the monolayer and the bilayer patches. (c) Result of digitally subtracting image (a) from (b) followed by multiplication by 8; $q_{\text{inner}}=1.97\pm 0.04 \text{ \AA}^{-1}$, $q_{\text{outer}}=2.15\pm 0.04 \text{ \AA}^{-1}$. The large white stripe is due to imperfect subtraction. (d) Commensurate oblique bilayer at a coverage near the second-layer completion. This pattern was taken on the same crystal in an earlier measurement.

The features of bilayer diffraction can be more clearly seen if the monolayer contribution is subtracted. In Fig. 1(c) we show an example of the subtraction from Fig. 1(b) of Fig. 1(a), followed by multiplication by 8. The resulting six groups of doublet arcs (see Fig. 2) is exactly what we see in Fig. 1(d), taken at a coverage near bilayer completion as inferred from the attenuation of the graphite (10) spot intensity. Again the q values are 1.97 and 2.15 \AA^{-1} for the inner and the outer arcs, respectively. They agree well with the positions of the lowest- and highest- q peak of the bilayer detected by neutron diffraction where another peak at $q=2.10 \text{ \AA}^{-1}$ is also seen,^{4,5} although its intensity in neutron diffraction is no more than 50% of that of the other two peaks. The detection of this third peak by neutron diffraction favors the oblique-bilayer model over the independent-triangular-layer model in which the two layers of D_2 molecules form mutually incommensurate triangular lattices.^{4,5}

Although only two peaks are observed in our LEED measurement, it is premature to link these peaks to two layers with vectors from different triangular lattices, because the azimuthal width of the corresponding spots, as wide as 0.24 \AA^{-1} , cannot be simply accounted for. In fact, by analyzing the spot shapes and positions, we are able to interpret the bilayer LEED pattern as originating from two mutually commensurate layers with an oblique unit cell. The oblique unit cell is shown in Fig. 3(a), where a_1 , a_2 , a_3 , α , β , and γ are its lattice parameters. To relate such an oblique cell to the observed LEED pattern, we note first that in the coverage regime that has been studied D_2 molecules grow on a graphite substrate in the layer-by-layer fashion.⁴ The significance of this fact is that by the time the second layer starts to grow, the monolayer has been so severely compressed that its lattice constant has become 3.415 \AA ,^{4,5} 20% smaller than

that of the $(\sqrt{3}\times\sqrt{3})R30^\circ$ structure or 4.6% smaller than that of the bulk hexagonal close-packed D_2 solid at zero pressure.⁴ The condensation of the second layer has been proposed to occur by formation of patches com-

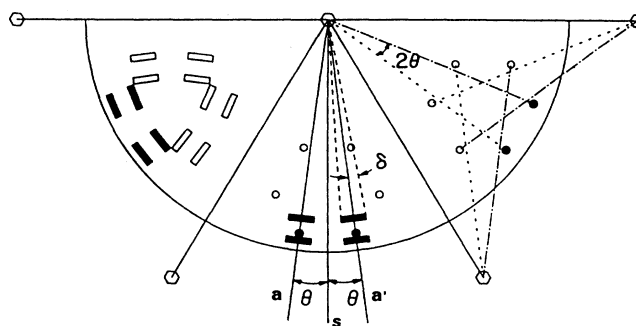


FIG. 2. Schematic drawing with geometry of both monolayer RIC and bilayer diffraction patterns. Monolayer RIC spots are indicated by circles with their size exaggerated. Solid and open circles indicate single- and double-scattering spots, respectively (Ref. 7). The bilayer arcs due to several spots overlapping are indicated by the boxes at the left and the center with their tangential length representing the azimuthal width of the arcs. The group of six spots at the right and the center illustrates the single and double scattering of the monolayer RIC phase with its $+\theta$ and $-\theta$ rotations indicated by dashed and dot-dashed lines. In the center, the spots and arcs illustrate the coexistence of the monolayer and bilayer with bilayer patches aligned close to the RIC direction. The spots and outer arcs are not resolved in Fig. 1(b). a and a' indicate two sets of RIC directions rotated $\pm\theta$ from the commensurate layer directions, respectively. δ is due to the misorientation of the oblique bilayer. Hexagons indicate graphite spots outside the field of view represented by the half-circle.

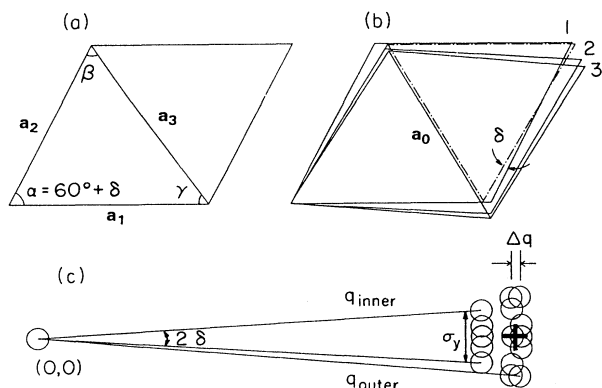


FIG. 3. Schematic of D_2 bilayer unit cells and spots. (a) The common oblique unit cell of the bilayer inferred from the LEED measurements. a_1, a_2, a_3 and $\alpha, \beta,$ and γ are listed in Table I. (b) Three different possible alignments labeled by 1, 2, and 3 of the oblique cell in (a) are shown along with the monolayer triangular cell (basis vector \mathbf{a}_0) indicated by dot-dashed lines. In the third alignment the diagonal line of the oblique cell 3 is parallel to that of the RIC cell. (c) The misorientation of the oblique cell and the symmetry operations turn one RIC spot (cross) to 18 spots (circles) which overlap each other partially to form three arcs. The size of the circles is larger than the resolution. In our LEED patterns the arc with intermediate q is absent. Note that the cross is not centered in any of the circles.

mensurate with the underlying first-layer portions, which adopt an oblique structure after promoting 1 out of 15 molecules to the second layer to release part of its lateral stress.⁴ Second, the deviation from the triangular symmetry by the bilayer patches can introduce structural defects, which may be energetically unfavorable, at the monolayer-bilayer boundaries. To minimize the number of occurrences of the defects, one side of the oblique cell may align with that of the triangular lattice with basis vector \mathbf{a}_0 . Clearly, three such alignments, namely, $\mathbf{a}_{1\parallel}\mathbf{a}_0$, $\mathbf{a}_{2\parallel}\mathbf{a}_0$, and $\mathbf{a}_{3\parallel}\mathbf{a}_0$, are possible, resulting in a range of misorientation of the bilayer diffraction spots (see Fig. 3). Therefore we attribute the azimuthal broadening of the LEED spots to such a misorientation. The observed LEED pattern is not due simply to any one of the oblique cell orientations, but to the sum of the three relatively rotated cells [see Figs. 3(b) and 3(c)], plus the symmetry operations upon them and the double scattering through first-order diffraction by the graphite plus first-order diffraction by the overlayer. The symmetry operations involved are threefold rotation and inversion with respect to the monolayer RIC symmetry direction, which has rotated $\theta = \pm 7.2^\circ$ from the commensurate direction.⁷ Thus the symmetry operations turn each spot to six spots when the lattice switches from triangular to oblique. The misorientation then triples the number of spots, which partially overlap one another to form three arcs, as shown in Fig. 3(c). However, only doublet arcs were seen in our LEED images; the third arc with intermediate q is missing due to the reasons we will discuss below.

The misorientation angle (see Figs. 2 and 3) is obtained

TABLE I. D_2 bilayer oblique structure inferred from LEED and from neutron diffraction.

Parameter	LEED	Neutron ^a
q_1 (\AA^{-1})	1.97(0.04) ^b	1.95
q_2	2.11(0.04) ^d	2.10
q_3	2.15(0.04) ^b	2.15
α (deg)	63.5(0.65) ^c	64.20
β	61.4 ^d	61.32
γ	55.1 ^d	54.48
a_1 (\AA)	3.56(0.09) ^d	3.584
a_2	3.33(0.05) ^d	3.325
a_3	3.63 ^d	3.678

^aData from Ref. 4 for bilayer completion.

^bIndicates direct LEED measurement.

^cIndicates angle inferred from by argument described in text.

^dCalculated from b and c.

by taking $\delta = \sigma_y / 2q_{\text{inner}}$, where $q_{\text{inner}} = 1.97 \text{ \AA}^{-1}$ is the magnitude of the diffraction vector for the inner spots, and σ_y is its azimuthal width (FWHM) measured from the corresponding profile. Figure 4 shows such an azimuthal profile with the monolayer contribution subtracted, taken after 5 pixel \times 5 pixel convolution filtering.⁸ The intrinsic width is left out because we have not found out a proper way to take it into account, due to the uncertainty in the line shape of the profile. The average σ_y inferred this way is $0.24 \pm 0.04 \text{ \AA}^{-1}$; thus $\delta = (3.5 \pm 0.7)^\circ$. On the other hand, if the misorientation is due to the deviation from the triangular symmetry, δ should be related to α by the expression $\delta = \alpha - 60^\circ$, where $\alpha > 60^\circ$ is the largest of the three lattice angles. Given these assumptions, by analyzing the spot profile and position, we are able to determine the lattice parameters for the bilayer oblique cell. The results are shown in Table I, which also contains data inferred by Wiechert from neutron diffraction.⁴ Agreement between the LEED and the neutron-diffraction measurement is excellent.

Throughout the above analysis we have been using the inner spots exclusively. The reason is that the outer spots are less appropriate to use, considering that they are close to or even outside the phosphor screen, and overlap

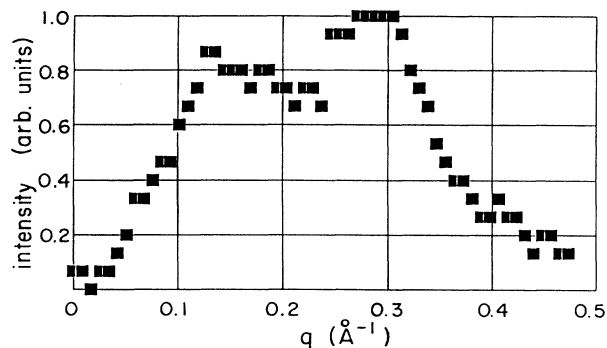


FIG. 4. Azimuthal profile of an inner spot taken from the LEED pattern shown in Fig. 1(c).

significantly with the monolayer RIC spots. The twin-peak feature shown in Fig. 4 is also quite typical for the outer spots independent of whether the monolayer contribution is subtracted. This may suggest that one of the three possible orientations is preferable, similar to the phenomenon of preferential nucleation observed in the condensation of the α phase of H_2 on graphite.⁷

The mutual modulation of D_2 molecules in two incommensurate triangular layers would in principle produce satellite peaks.⁶ However, it has not yet been explored whether the third peak in neutron diffraction could be a satellite due to such a modulation. Knowledge of the azimuthal orientation makes it possible to investigate the position of the satellite peaks. To explain the azimuthal broadening of the LEED spots, the two mutually modulated triangular lattices would have to adopt the geometry shown in Fig. 5, where $q_1 = q_{\text{inner}}$ and $q_{10} = q_{\text{outer}}$ are 3.5° from each other. (After mirror reflection this would give a maximum total width of $2\delta = 7.0^\circ$ as measured.) The modulation wave vector is represented by τ . Overall, ten first-order satellites are possible due to the sixfold symmetry of the triangular lattices. Yet none of these satellite scattering vectors has the correct magnitude to reproduce the third peak at $q = 2.10 \text{ \AA}^{-1}$ observed by the neutron diffraction; the values of q_1 through q_{10} in units of \AA^{-1} are 1.97, 1.96, 2.15, 2.34, 2.35, 2.17, 2.01, 1.80, 1.77, and 2.15.

As pointed out above, the third peak detected by neutron diffraction is absent in our LEED measurement. We offer the following reasons: (a) even if the spots were present near $q = 2.10 \text{ \AA}^{-1}$ in the monolayer-bilayer coexistence regime, we would not be able to resolve them from the stronger RIC spots at $q = 2.12 \text{ \AA}^{-1}$; (b) above the bilayer completion, although the RIC spots were not present, the intensity of all LEED spots became weaker while the diffuse background increased substantially, making the intensity of the third peak below our detec-

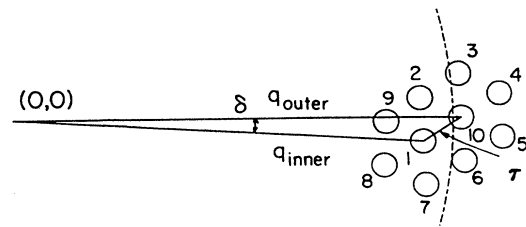


FIG. 5. Satellite spots due to the modulation of the two incommensurate triangular lattices whose scattering vectors are $\delta = 3.5^\circ$ apart. τ is the modulation wave vector. Spots 1 and 10 are the first-order diffraction spots from the scattering vectors q_{inner} and q_{outer} , respectively. q_{outer} aligns with one of the RIC directions. None of the other satellites can account for the third peak observed by the neutron diffraction, which is located at the radius given by the dashed line.

tion limit; and (c) the perpendicular momentum transfer in LEED is quite different than at the leading edge of the neutron measurements,¹¹ thus possibly changing the relative intensities of the three peaks. We hope the results presented here will stimulate more research on the growth and structure of the quantum systems in terms of how the commensurability, symmetry, and orientational epitaxy will vary with the layer-by-layer growth.

We gratefully acknowledge helpful communications from Professor H. Wiechert, Professor L. Bruch, and Professor J. Phillips. Dr. D. Zehner provided us graphite single crystals. Dr. J. Cui kindly allowed us to refer to his unpublished LEED images. Dr. V. Eden developed the image acquisition and processing system that has been used here. This work was supported by NSF Grants Nos. DMR-88-14180 and DMR-91-19701.

¹For a review of computer simulations and experimental data for argon and methane bilayers, see J. M. Phillips and Neil Shrimpton, *Phys. Rev. B* **45**, 3730 (1992).

²H. J. Lauter, H. Godfrin, V. L. P. Frank, and P. Leiderer, in *Phase Transitions in Surface Films 2*, Vol. 267 of *NATO Advanced Study Institute, Series B: Physics*, edited by H. Taub, G. Torzo, H. J. Lauter, and S. C. Fain, Jr. (Plenum, New York, 1991), p. 135.

³H. J. Lauter, H. P. Schildberg, H. Godfrin, H. Wiechert, and R. Haensel, *Can. J. Phys.* **65**, 1435 (1987).

⁴H. Wiechert, in *Excitations in Two-Dimensional and Three-Dimensional Quantum Fluids*, edited by A. G. F. Wyatt and H. J. Lauter (Plenum, New York, 1991), p. 499.

⁵H. P. Schildberg, H. J. Lauter, H. Freimuth, H. Wiechert, and R. Haensel, *Jpn. J. Appl. Phys.* **26**, Suppl. 26-3, 343 (1987).

⁶J. P. McTague and A. D. Novaco, *Phys. Rev. B* **19**, 5299 (1979).

⁷J. Cui and S. C. Fain, Jr., *Phys. Rev. B* **39**, 8628 (1989).

⁸W. Liu and S. C. Fain, Jr., *J. Vac. Sci. Technol. A* **10**, 2231 (1992).

⁹J. Cui, S. C. Fain, Jr., H. Freimuth, H. Wiechert, H. P. Schildberg, and H. L. Lauter, *Phys. Rev. Lett.* **60**, 1848 (1988); **60**, 2704(E) (1988).

¹⁰In some unpublished measurements J. Cui acquired bilayer D_2 LEED images that appear very similar to those presented here; J. Cui (private communication).

¹¹S. C. Fain, Jr. and H. You, in *The Structure of Surfaces*, edited by M. A. Van Hove and S. Y. Tong (Springer-Verlag, Berlin, 1985), p. 413.

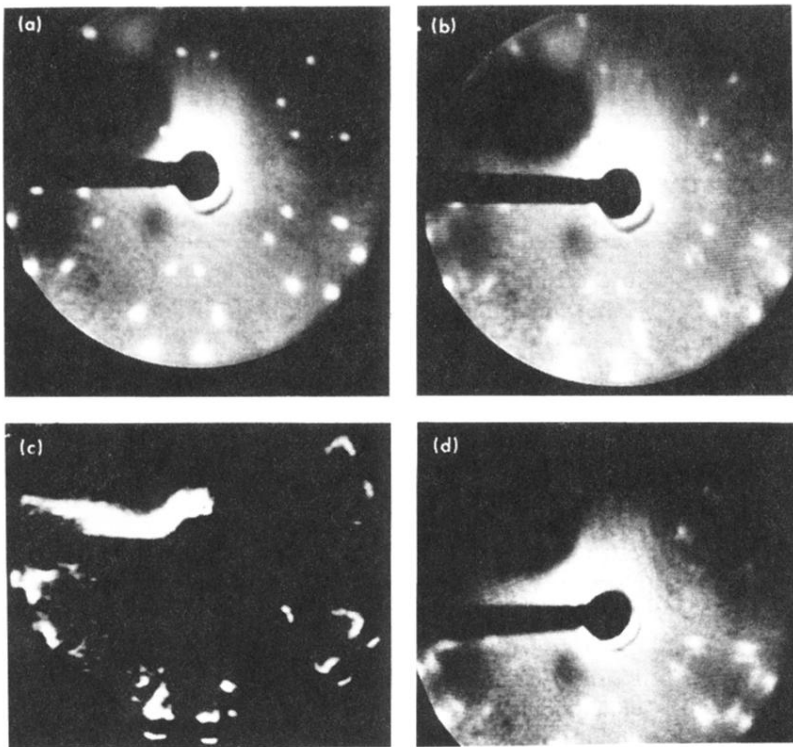


FIG. 1. Photograph of LEED patterns near 4.5 K for 63.2-eV electron energy. (a) Rotated incommensurate triangular solid phase near monolayer completion with the lattice constant $d=3.41\pm 0.04 \text{ \AA}^{-1}$ and the rotational angle $\theta=(7.2\pm 0.5)^\circ$. (b) Coexistence of the monolayer and the bilayer patches. (c) Result of digitally subtracting image (a) from (b) followed by multiplication by 8; $q_{\text{inner}}=1.97\pm 0.04 \text{ \AA}^{-1}$, $q_{\text{outer}}=2.15\pm 0.04 \text{ \AA}^{-1}$. The large white stripe is due to imperfect subtraction. (d) Commensurate oblique bilayer at a coverage near the second-layer completion. This pattern was taken on the same crystal in an earlier measurement.